

# $\sigma$ and $\pi$ -band dispersion of graphite from polarized resonant inelastic X-Ray scattering measurements

A. V. Sokolov, E. Z. Kurmaev, J. MacNaughton<sup>+</sup>, A. Moewes<sup>+</sup>, N. A. Skorikov, L. D. Finkelstein

*Institute of Metal Physics Ural Division RAS, 620219 Yekaterinburg GSP-170, Russia*

<sup>+</sup>*Department of Physics and Engineering Physics,  
University of Saskatchewan, Saskatoon, Saskatchewan S7N 5E2, Canada*

Submitted 24 December 2002

Resonant inelastic X-Ray scattering of highly oriented pyrolytic graphite (HOPG) is observed above the C 1s threshold at different polarization angles. It is shown that combining the polarization and excitation energy dependence of X-Ray emission spectra makes it possible to perform the quantitative band mapping selective to the chemical bonding ( $\sigma$  and  $\pi$ ).

PACS: 78.70.-g, 71.25.Tn

Non-resonant X-Ray emission can exhibit radiation anisotropy or linear dichroism in anisotropic crystals [1–3]. It is shown that using the orientation dependence of polarized X-Ray emission spectra (XES) of single crystals with low symmetry, that the additional information about the anisotropy of chemical bonding parameters can be obtained [4]. Conversely, it is demonstrated recently that quantitative band mapping can be performed for occupied electronic states in SiC [5], diamond, graphite and MgB<sub>2</sub> [6] with the help of resonant inelastic X-Ray scattering (RIXS) measurements. In this paper we combined both polarization dependence of X-Ray absorption spectrum (XAS) and RIXS measurements to perform quantitative band mapping selective to chemical bonding. The excitation energy dependence of C  $K\alpha$  XES ( $2p \rightarrow 1s$  transition) of highly oriented pyrolytic graphite was measured above the C 1s-threshold for 0–10 eV at two different polarization geometries. The results were compared with specially performed band structure calculations of graphite.

The X-Ray fluorescence measurements were performed on Beamline 8.0 at the Advanced Light Source (ALS) at the Lawrence Berkeley National Laboratory using a fluorescence endstation described in details elsewhere [7]. Emitted radiation was measured using a Rowland circle type spectrometer with a large spherical grating and a photon-counting area detector. Total experimental resolution in the carbon  $K\alpha$  X-Ray emission region was 0.3 eV FWHM. The bandwidth of the incident photons was varied between 500 meV and 1 eV. The C 1s XAS was measured in the total electron yield mode. The fluorescence measurements were made at the beamline using a depolarized configuration, (which means that the vector  $\mathbf{E}$  of the incidence beam lies in

scattering plane, i.e. we used p-polarization) as well as having the direction of the emitted photons perpendicular to the incidence one. Two geometries were used:  $\alpha = 85^\circ$  (which is close to the normal incidence) and  $\alpha = 25^\circ$  (which is close to the grazing incidence). The variable  $\mathbf{c}$  is the sample normal and  $\alpha$  is the angle between incident photons and the surface of the sample.

We have used a self-consistent linearized muffin-tin orbital (LMTO) method within the local density approximation (LDA) for the band structure calculation of graphite (TBLMTO-47 computer code [8]). The tetrahedron method was used to calculate the dispersion curves  $E(\mathbf{k})$  with 1152  $\mathbf{k}$ -points.

Initially, we studied the polarization dependence of the near-edge X-Ray absorption fine structure of graphite. The transition matrix element  $M$  in the X-Ray absorption process contains the scalar product of the polarization vector of the incoming photon,  $\mathbf{E}$  and the position vector of the electron,  $\mathbf{r}$ . The expression is,

$$M = \langle \varphi_{1s} | \mathbf{E} \cdot \mathbf{r} | \varphi_f \rangle,$$

where  $\varphi_{1s}$  is the wave function of the C 1s core electron and  $\varphi_f$  is the wave function of the final state into which the 1s electron is excited [9]. The dipole transition operator  $\mathbf{E} \cdot \mathbf{r}$  projects orbitals along the direction of the polarization vector. Therefore, the orbital-symmetry dependent absorption spectra can be obtained using linearly polarized synchrotron radiation. In highly oriented pyrolytic graphite the  $\mathbf{c}$  axis coincides with the sample normal. This means that the  $p_z$  or out-of-plane orbitals ( $\pi^*$ -bands) are mainly excited at  $K$ -edges, or when  $\mathbf{E} \parallel \mathbf{c}$ . Similarly, the  $p_{x,y}$  or in-plane orbitals ( $\sigma^*$ -bands) are preferentially excited when  $\mathbf{E} \perp \mathbf{c}$ .

Fig.1a shows C 1s XAS of graphite measured at different incidence angles ( $\alpha = 85^\circ$  and  $\alpha = 25^\circ$ ) and

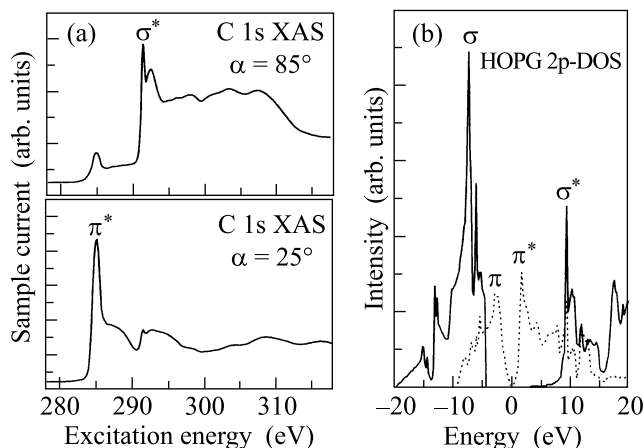


Fig.1. (a) C 1s XAS of graphite measured at polarization angles  $\alpha = 25^\circ$  and  $85^\circ$ ; (b) C 2p-DOS separated for  $\sigma$  and  $\pi$  states

Fig.1b shows the 2p-DOS calculations separately for  $\pi$  and  $\sigma$  bonds. As observed, the fine structure of C 1s XAS is very sensitive to the incidence angle. The absorption peak located at 285 eV caused by the dominant  $\pi^*$ -states [10] is enhanced at  $\alpha = 25^\circ$ . Alternately, at normal incidence ( $\alpha = 85^\circ$ ) the  $\sigma^*$ -states are mainly probed and the absorption peak located at 291.5 eV has the highest intensity.

Excitation energy dependence of the X-Ray emission spectra measured for different incidence angles ( $\alpha = 25^\circ$  and  $\alpha = 85^\circ$ ) is presented in Figs.2–3. The excitation energies were selected according to features (a–h) in the C 1s XAS (indicated by arrows in Figs.2, 3). Excitation energies a–h have the same values for both incidence angles. The intensities of each emission spectrum have been normalized to the incident flux.

Abiding by the dipole selection rules, the carbon  $K\alpha$  XES of graphite probes the occupied 2p-states. This process depends strongly on the excitation energy of incoming photons and varies significantly for the two angles chosen.

When excitation energy shifts above the  $K$ -edge, the fine structure of C  $K\alpha$  XES changes dramatically. Instead of linear dispersion, the peaks move in a nonlinear fashion. Some of these features move in a manner opposite to the increasing excitation energy. For interpretation of these spectra we are using the concept [11] that the absorption- emission process should be treated as a single inelastic scattering process with well defined crystal momentum conservation for both the photoelectron and the hole in the valence band. This indicates

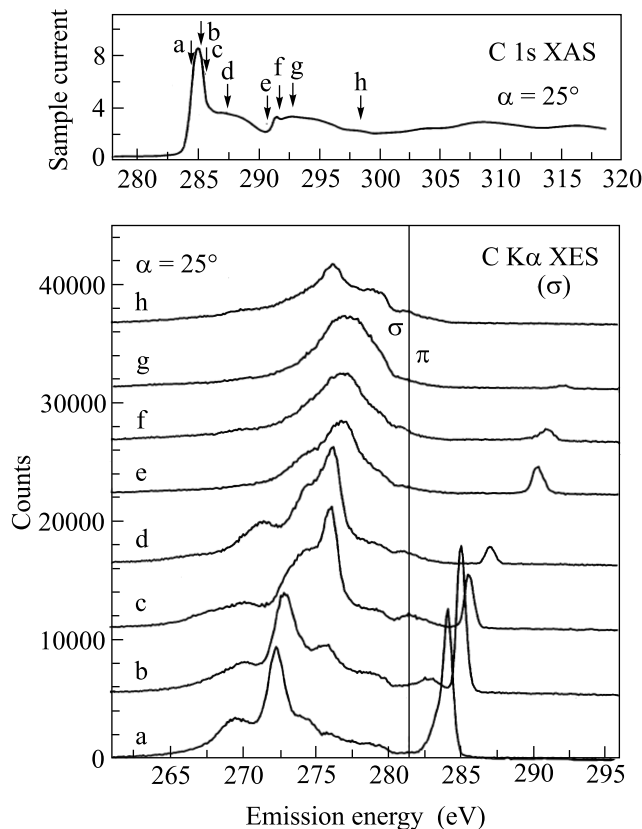


Fig.2. Excitation energy dependence of C  $K\alpha$  XES of graphite measured for incidence angle  $\alpha = 25^\circ$

that when a core electron is promoted to the conduction band with a certain crystal momentum, a resulting emission from the valence band at the same point in the Brillouin zone will be induced.

To compare presented spectra for two angles one should take into account the contribution of  $\pi$ - and  $\sigma$ -states to the emission process is determined by the direction in which we register emitted photons. If this outgoing direction is parallel to the  $c$  axis, then the polarization vector of emitted photons is parallel to the sample surface and thus the dominant component is  $\sigma$ . In the opposite situation, when the direction of departing photons is perpendicular to  $c$  axis, the polarization vector of the emitted photons is either parallel to the  $c$  direction or to one of the directions in the sample surface, producing both  $\pi$  and  $\sigma$  contributions. Our results indicate that the direction of registration is perpendicular to the incident direction. Thus, for incidence angle  $\alpha = 25^\circ$  (close to grazing incidence) the direction of registration of the emitted photons is nearly parallel to the  $c$  axis and the dominant component is  $\sigma$ . For  $\alpha = 85^\circ$  (close to normal incidence) the direction of registration is nearly perpendicular to the  $c$  axis and we have both  $\pi$  and  $\sigma$  components.

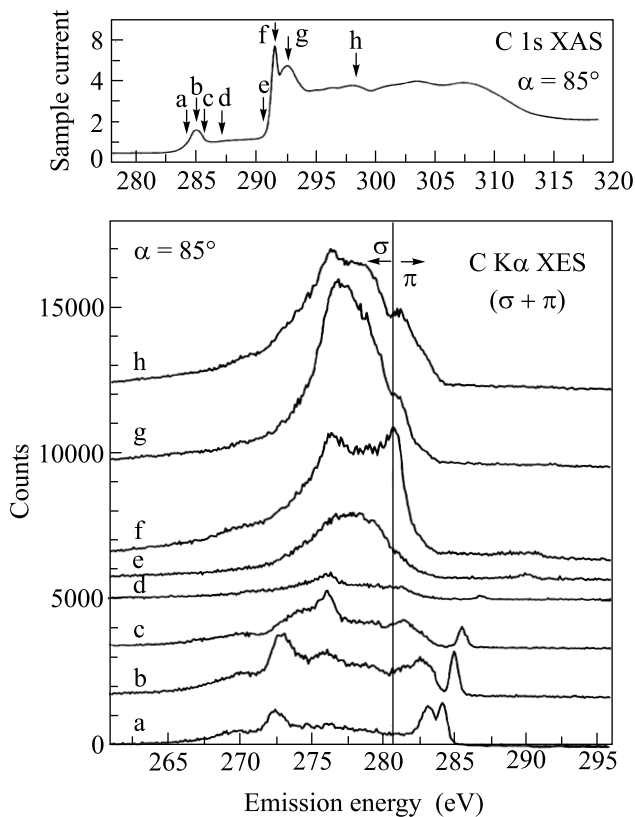


Fig.3. Excitation energy dependence of C  $K\alpha$  XES of graphite measured for incidence angle  $\alpha = 85^\circ$

All the features of the RIXS for  $\alpha = 25^\circ$  are results of the  $\sigma$  component, with the exception of those in the high-energy field of the valence band. These  $\pi$  states for excitation energies  $b-d$  appear because the registration of emitted photons is not strictly parallel to  $c$  axis. For  $\alpha = 85^\circ$  and both  $\pi$  and  $\sigma$  components are allowed in the emission process, the  $\pi$  (high-energy) features are more considerable in the whole excitation energy range. The strong elastic peaks corresponding to  $\alpha = 25^\circ$  occur because of their localized character and the strong deviation from grazing incidence that results in permission of  $\pi^*$  states in the emission process.

To construct the experimental dispersion curves from selectively excited X-Ray emission spectra we have used the procedure described in Refs.[5, 6]. According to this procedure, the top of the valence band corresponding to the calculated zero in the energy scale is related to XPS C  $1s$  binding energy of 284.5 eV measured for graphite [12]. For the band mapping procedure we used only the inelastic part of the spectra. The possible values of the  $\mathbf{k}$ -vector for excited C  $1s$  electrons are determined by the intersection of the selected excitation energy and the calculated dispersion curves for the  $2p$ -vacant states. Using  $\mathbf{k}$ -momentum conservation,

vertical lines from intersection points are drawn down on dispersion curves for occupied states. The occupied states revealed by features in the carbon  $K\alpha$  XES for selected excitation energies can be indicated by horizontal lines on the dispersion curves for occupied  $2p$ -states. The intersection points of horizontal and vertical lines give the experimental points on dispersion curves for the occupied states.

As a result, the quantitative band mapping selective to the chemical bonding ( $\pi$  and  $\sigma$ ) was realized for  $\alpha = 25^\circ$  (Fig.4). The obtained results show a good

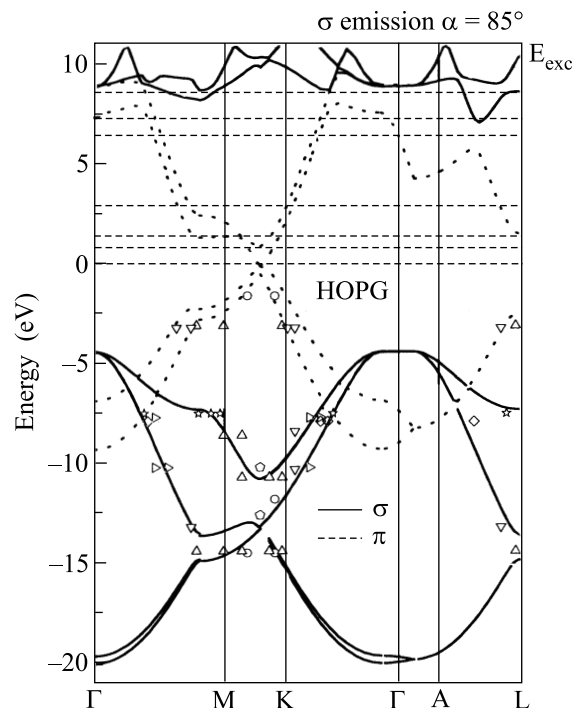


Fig.4. Band mapping using resonant inelastic X-Ray scattering, lines are calculated band structure and dots are the experimental results (for  $\alpha = 25^\circ$ . Values of  $E_{exc}$  are:  $\star$  292.9,  $\diamond$  291.7,  $\triangleright$  290.8,  $\nabla$  287.3,  $\Delta$  285.8,  $\circ$  285.2,  $\circ$  285.4)

agreement for experiment (points) and calculated dispersion curves for occupied  $\pi$  (dotted lines) and  $\sigma$  (solid lines) states of graphite which are located at the top and the bottom of the valence band, respectively.

In conclusion, we have shown that resonant inelastic X-Ray scattering spectra measured at different incidence angles can be used for quantitative band mapping selective to the chemical bonding using  $p$ -polarization of the incoming photons. This technique has advantages with respect to angle-resolved photoemission because of higher sensitivity to the chemical bonding and a greater potential for probing the  $\mathbf{k}$ -resolved electronic structure of layered materials.

This work was supported by the Russian Foundation for Basic Research (Projects # 00-15-96575) and the National Sciences and Engineering Research Council (NSERC). The work at the Advanced Light Source at Lawrence Berkeley National Laboratory was supported by U.S. Department of Energy (Contract # DE-AC03-76SF00098).

1. I. B. Borovskii, V. I. Matiskin, and V. I. Nefedov, *J. Physique* **32**, C4-207 (1971).
2. V. M. Cherkashenko, E. Z. Kurmaev, and V. L. Volkov, *J. Electr. Spectr. Relat. Phenom.* **28**, 1 (1982); S. P. Freidman, V. M. Cherkashenko, V. A. Gubanov et al., *Z. Phys.* **B46**, 31 (1982).
3. G. Drager and O. Brummer, *Phys. Stat. Sol. (b)* **124**, 300 (1984).
4. Chr. Beyreuther, R. Hierl, and G. Wiech, *Berichte der Bunsen-Gesellschaft* **79**, 1082 (1975).
5. J. Luning, J.-E. Rubensson, C. Ellmers et al., *Phys. Rev.* **B56**, 13147 (1997).
6. A. V. Sokolov, E. Z. Kurmaev, S. Leitch et al., to be published.
7. J. J. Jia, T. A. Callcott, J. Yurkas et al., Perera, *Rev. Sci. Instrum.* **66**, 1394 (1995).
8. O. K. Anderson, *Phys. Rev.* **B12**, 3060 (1975).
9. J. Stohr, *NEXAFS Spectroscopy*, Springer, Berlin, 1992.
10. D. M. Gruen, A. R. Krauss, C. D. Zuiker et al., *Appl. Phys. Lett.* **68**, 1640 (1996).
11. Y. Ma, N. Wassdahl, P. Skytt et al., *Phys. Rev. Lett.* **69**, 2598 (1992).
12. J. F. Moulder et al., *Handbook of X-Ray Photoelectron Spectroscopy*, Perkin-Elmer Corp., Eden Prairie, MN, 1992.